First-principles calculations of heat capacities of ultrafast laser-excited electrons in metals

Emile Bévillon, Jean-Philippe Colombier, Vanina Recoules, Razvan Stoian

Available online at www.sciencedirect.com

ScienceDirect

Applied Surface Science 00 (2015) 1–7

Applied Surface Science

First-principles calculations of heat capacities of ultrafast laser-excited electrons in metals

E. Bévillon[a], J.P. Colombier[a,*], V. Recoules[b], R. Stoian[a]

[a]*Laboratoire Hubert Curien, UMR CNRS 5516, Université de Lyon, Université Jean Monnet 42000, Saint-Etienne, France*
[b]*CEA-DIF, 91297 Arpajon, France*

Abstract

Ultrafast laser excitation can induce fast increases of the electronic subsystem temperature. The subsequent electronic evolutions in terms of band structure and energy distribution can determine the change of several thermodynamic properties, including one essential for energy deposition; the electronic heat capacity. Using density functional calculations performed at finite electronic temperatures, the electronic heat capacities dependent on electronic temperatures are obtained for a series of metals, including free electron like, transition and noble metals. The effect of exchange and correlation functionals and the presence of semicore electrons on electronic heat capacities are first evaluated and found to be negligible in most cases. Then, we tested the validity of the free electron approaches, varying the number of free electrons per atom. This shows that only simple metals can be correctly fitted with these approaches. For transition metals, the presence of localized *d* electrons produces a strong deviation toward high energies of the electronic heat capacities, implying that more energy is needed to thermally excite them, compared to free *sp* electrons. This is attributed to collective excitation effects strengthened by a change of the electronic screening at high temperature.

Keywords: Ultrashort laser; Femtosecond laser-excited electrons; First-Principles calculations; Electronic Heat Capacities.

1. Introduction

Material response to intense laser excitation is the subject of important research activities, and recent advances have revealed the determinant role of primary excitation events. Their accurate comprehension is necessary to correctly describe ultrafast structural dynamics [1, 2], phase transitions [3, 4], nanostruture formation [5], ablation dynamics [6, 7], or strong shock propagation [8]. The interplay between ultrafast excitation and resulting excited material response still requires a comprehensive theoretical description for highly excited solid materials. Ultrashort laser irradiation produces a strong inhomogeneous heating of electrons that rapidly exchange energy through electron-electron collisions, leading the electronic subsystem to a thermalized state which is intimately related to the electronic structure of the material. This fast heating of the electronic subsystem leads in turn to a significant electron-phonon nonequilibrium, as the energy of the laser pulse is deposited before relaxation takes on and the material starts dissipating energy by thermal or mechanical ways.

During intense laser exposition, the irradiated material undergoes successive stages of extreme constraints, starting from the inhomogeneous excitation of electrons, the swift rise of electronic temperature and electronic pressure after thermalization of the electronic subsystem on the tens of femtosecond timescale [9]. These rapid processes

*Corresponding author
Email address: jean.philippe.colombier@univ-st-etienne.fr (J.P. Colombier)

are followed by the rise of the ionic temperature associated to thermally-triggered phase transitions, before ablating or returning to ambient conditions from further energy dissipations occurring at larger timescale. The accurate knowledge of these rapidly evolving conditions, in intensity and time, is of importance as they modify material properties. Evolution of electronic and ionic temperatures, T_e and T_i respectively, are generally calculated with the two-temperature model [10, 11] which involved transient parameters such as electronic heat capacity, electron-phonon coupling strength, thermal conductivity, electronic pressure and material absorptivity.

The basic underlying assumption in the two-temperature model is that the electron subsystem consists of a thermalized population of a certain amount of electrons, a condition easily fulfilled in ablation processes conditioned by high electronic temperatures [7]. The energy evolution is determined by photon absorption, energy accumulation and thermal/mechanical transport (involving electron-electron and electron-phonon interaction) based on nonequilibrium dynamics. The effective number of charge carriers taking part in absorption, storage and dissipation of the energy has to be carefully evaluated to give a correct description of the evolution of the corresponding transient properties. A certain amount of free electrons responds collectively to the laser field through intraband transitions, associated to one-electron excitation corresponding to interband transitions. Modelling this absorption stage is rather complex, particularly for ultrashort laser irradiation as it initiates a strong charge disorder. The consequence of a nonthermal electron-ion population on the electronic energy storage is also of major importance. Finally, thermal and mechanical transports are often described by the concept of "free carriers", since mobility is required for these processes. Electronic pressure has been seen to follow a free electron like behavior at high T_e, even at solid density [12]. The electronic heat capacity C_e plays an important role since it connects the quantity of absorbed energy to the rise of the electronic temperature of the system, regardless to energy dissipation processes. Electronic heat capacities have been derived from post-treatment of first-principles calculations where electronic excitation was not fully taken into account [13, 14]. Further, these quantities have been refined from density functional calculations dependent on the electronic temperature [12, 15].

In this paper, the electronic heat capacity of a series of transition metals is discussed in detail, first according to various modelling conditions, considering the effect of the exchange and correlation energy functionals and then the effect of semicore electrons. C_e are then discussed in the framework of a free electron approach in order to evaluate the impact of d electrons of transition metals on this crucial thermodynamic quantity.

2. Calculation details

The modelling of Al, Ni, Cu, Au, Ti and W metals is performed with the code Abinit [16], which is based on plane-waves description of the wavefunctions. Calculations are carried out within the density functional theory [17, 18] extended to finite electronic temperatures [19]. Projector augmented-waves atomic data [20] are used to take into account the effects of nuclei and core electrons. A cutoff energy of 40 Ha is applied to restrict the number of plane-waves and the Brillouin zone is meshed with a $30\times30\times30$ k-point grid using the Monkhorst-Pack method [21]. The local density approximation (LDA) [22] and the generalized gradient approximations (GGA) [23] are used with or without semicore electrons depending on the metals, in order to evaluate effects of semicore electronic states on computed properties. Computations are realized at the theoretical equilibrium lattice parameter of the crystal phase obtained at $T_i = 0$ K. Thus, electronic temperatures from 10^{-2} to 10^5 K are applied through a Fermi-Dirac distribution of electrons within a cold lattice. Such high T_e are conjectural and interrogate about phase stabilities. As we need to achieve a high temperature asymptotic behavior in this study, we will assume here that time and spatial conditions are not fulfilled for phase transitions to occur.

The calculated electronic heat capacity is derived from the variation of the internal energy E with respect to the electronic temperature as $C_e = \partial E/\partial T_e$. This thermodynamic quantity is computed for a series of metals at various T_e using LDA or GGA functionals with or without semicore electrons. Results are provided in Fig. 1 alongside the values of Lin *et al.* obtained from electronic structures calculated at $T_e = 0$ K [14]. At a first glance, the agreement between their results and ours is rather good for the low temperature range, the deviations appear at T_e above 4×10^4 K, where electronic structures start to react significantly to the heating of the electronic subsystem. In particular, transition and noble metals having a d-block within their valence band are sensitive to Fermi smearing, impacting d electron population, that induces a change of the electronic screening which in turn produces a significant energy shift of the d-block [4, 12]. At high temperature, this produces a significant effect on the band structure, with consequences on the electronic heat capacities. The effect of exchange and correlation functional appears to be weak on computed C_e.

The LDA method generally provides lower equilibrium parameters than the GGA, leading to slightly higher electronic electronic heat capacities per unit of volume.

The effect of semicore electronic states are also evaluated and Fig. 1(f) shows clearly that $4f$ semicore electrons of W have an impact at high T_e. Despite the fact that the 14 f electrons lie on deep states, around 19 eV below the valence band, they are significantly impacted by the increase of T_e starting from 4×10^4 K. For Al, Ni and Cu, the highest semicore electronic states correspond to $2p$ ones, they are located 50 eV below the valence band and are weakly impacted, even at high T_e. Nevertheless, a small effect of semicore electronic states is noticeable, with stronger C_e values for Al and Ni and lower values for Cu, compared to calculations where semicore states are not considered. With first semicore electronic states located at −27 eV for Ti, a significant effect of semicore electronic states is likely effective at high T_e. A deeper investigation of the evolution of the electronic semicore states when T_e increases shows that they are as sensitive as the d band to changes of the electronic screening. Depopulation or population of the d band with T_e, induces either a decrease or an increase of the electronic screening which is signalled by changes of the Hartree energy, and which is effective on localized electrons of the system, from d electrons to semicore electrons. As an example, at 10^5 K the energy of the electronic semicore states are shifted for −3 eV for $2p^6$ electrons of Ni, −8 eV for $2p^6$ electrons of Cu, 2 eV for $2p^6$ and −4 eV for $4f^{14}$ electrons of W. Semicore states are not shifted for Al, since this metal does not have a d block in its valence band. The shifts of these deep electronic states follow the changes of the electronic screening as discussed in Ref. [12]. This indicates that the evolution of the electronic screening, induced by changes of the electronic population of the d block, propagate to the localized charge density corresponding to semicore electronic states.

Nonetheless, due to the low energy of electronic semicore states and their corresponding electronic densities more localized around the nucleus, semicore electrons thermalize slower than valence electrons [24]. According to this consideration, the following part of this study relies on PAW atomic data without semicore electrons, at least when they are not needed for a good description of general properties. This implies that the GGA functional is used for Al, Ni, Cu and the LDA for Au, neglecting the effects of semicore electrons. For Ti and W, the GGA functional is used with semicore electrons but without the $4f^{14}$ electrons of W.

3. Electrons involved in C_e

In the framework of a free electron model, C_e has a linear behavior at low temperature that can be modelled by a low temperature limit $C_e^l = \pi^2 N_f n_i k_B^2 T_e / 2\varepsilon_F$ and saturates at high temperature to a non-degenerate limit $C_e^h = 3/2 N_f n_i k_B$. Here, N_f represents the number of free electrons per atom, n_i the ionic density, k_B the Boltzmann constant and ε_F the Fermi level. In Fig. 2, C_e is plotted for all the studied metals, and free electron like limits are presented at low and high temperatures. These limits are fitted to C_e with an effective number of electrons N_e^{eff}, provided in the figure, such as $N_f = N_e^{eff}$. At low temperature, the fit is performed up to an electronic temperature of 5×10^3 K, while at higher temperature, the corresponding number of electrons is a rough estimation since the asymptotic limit is not reached for most of the studied systems.

In order to facilitate the comparison between the number of effective electrons N_e^{eff} required to fit C_e and classical free electron numbers, their respective values are reported in Table 1. N_f from Ref. [25] are not designed to evolve with the increase of T_e due to the rigid definition of this number, which is based on the most extended orbitals of the electronic configuration of the isolated atoms. On the contrary, temperature dependent $N_f(T_e)$ are obtained from extended-orbital overlapping considerations based on temperature-dependent electronic structure calculations [12], that allows electronic transfer between bands and Fermi-Dirac redistribution of electrons. Unsurprisingly, both free electron numbers remain quite close at low temperature, with a significant increase of $N_f(T_e)$ compared to N_f when the temperature increases. This originates in the redistribution of electrons from localized d electronic states to delocalized electronic states of higher energies.

As expected, both low and high temperature approaches perfectly catch the limit behaviors of the free electron metal Al, with an effective number of electrons equals to 3, in agreement with the numbers of free electrons expected for this element. However, the number of effective electrons, needed to correctly fit the complex evolution of electron heat capacities of transition metals, can be very high and somewhat unrealistic. At low electronic temperature, an important gap is observed between N_e^{eff} and expected N_f for transition metals. For W, the number of effective electrons equals the number of electrons in the valence band, while for Ti N_e^{eff} is even higher than available electrons

in the valence band. Reducing the temperature interval where the fit is applied does not modify significantly N_e^{eff}, except in the case of Ni where this number reaches 19 electrons to catch the particularly strong slope of C_e at $T_e = 300$ K [13]. In all cases, N_e^{eff} remains remarkably high compared to the number of free electrons classically used.

Table 1. Typical free electron numbers N_f from Ref. [25] and temperature-dependent free electrons numbers $N_f(T_e)$ from Ref. [12], with estimated number of effective electrons N_e^{eff} required to fit C_e in the low and high temperature regimes.

	Al	Ni	Cu	Au	Ti	W
			$T_e = 5 \times 10^3$ K			
N_f	3	2	1	1	2	2
$N_f(T_e)$	3.0	1.5	1.9	2.4	1.3	2.1
N_e^{eff}	3	5	5	5	6	6
			$T_e = 10^5$ K			
N_f	3	2	1	1	2	2
$N_f(T_e)$	3.0	2.9	3.3	4.2	2.2	3.5
N_e^{eff}	3	5	7	8	6	6

From the low temperature to the high temperature regime, N_e^{eff} values evolve differently from a material to an other, remaining constant for Ni, Ti and W, while increasing for Cu and Au. These values still strongly exceed typical values of N_f, even if the temperature dependence is considered, signalling a collective effect of d-electrons.

4. Discussion

The significant differences between N_e^{eff} and the typical values of N_f at low and high temperatures, demonstrate the inability of asymptotic limits derived from free electron approaches to grasp the complex behavior of transition metals, which relies on the presence of localized d electrons. Indeed, these localized electrons also contribute to the change of the electronic heat capacity, through the change of free energy in the system as T_e increases. The electronic heat capacity informs about the amount of energy needed to rise the electronic temperature of a given system. The fast deviation toward high values of C_e observed for transition metals, which is illustrated by values of N_e^{eff} much higher than the classical values of N_f, implies that the energy required to heat the localized d electrons is higher than the energy needed to heat free electrons. Moreover, non-linear evolution of N_e^{eff} with the increase of T_e also indicates a complex impact of d electron contribution to C_e. Finally, previous studies showed that the change of d electron numbers with T_e modifies the electronic screening that in turn induces an energy shift of the d-block affecting all localized d electrons [4, 12]. Consequently, the effect of d electrons on C_e has to be considered as a collective effect of the overall localized d electrons. Thus, the number of electrons to be considered in the electronic heat capacity limits at low and high temperature should be reevaluated, according to an activity coefficient applied to the different types of electrons:

$$N_e^{eff} = \alpha_f N_f + \alpha_d N_d + \alpha_{sc} N_{sc} \tag{1}$$

where N_f represents the number of free electrons as defined before, $N_d = N_v - N_f$ is the number of d electrons, with N_v being the number of valence electrons, and N_{sc} is the number of semicore electrons. α_i stands for the activity coefficient for each category of electrons. α_f is set to the value of 1 for all metals as it corresponds to the free electron approaches. Since PAW atomic data used here exclude most of the semicore electrons and N_{sc} is set to 0. Considering that N_e^{eff} is equal to the values provided in Fig. 2 it is then possible to deduce the activity coefficients of d electrons for all the transition metals at low and high temperatures from $\alpha_d = (N_e^{eff} - N_f)/N_d$. This is solved within a temperature dependence of free electron numbers and d electrons numbers that are presented in Table 2. The corresponding activity coefficients of d electrons are provided in Fig. 3.

As expected, α_d for Al remains equal to 0 due to the absence of d electrons. For Ni, Cu and Au, the coefficient values are in the range of 0.2-0.5, with an increase for Cu and Au and a decrease for Ni when T_e increases. These

Table 2. Temperature-dependent free electron numbers $N_f(T_e)$ from Ref. [12] and corresponding number of localized d electrons $N_d(T_e) = N_v - N_f(T_e)$ in the low and high temperature regime.

	$T_e = 5 \times 10^3$ K		$T_e = 10^5$ K	
	$N_f(T_e)$	$N_d(T_e)$	$N_f(T_e)$	$N_d(T_e)$
Al	3.0	0.0	3.0	0.0
Ni	1.5	8.5	2.9	7.1
Cu	1.9	9.1	3.3	7.7
Au	2.4	8.6	4.2	6.8
Ti	1.3	2.7	2.2	1.8
W	2.1	3.9	3.5	2.5

significant activity coefficients of d electrons - that applies on all localized d electrons - imply that the response of these electrons is strong, even when the Fermi smearing weakly affects them at low temperature, as for Cu and Au. On the contrary, α_d reach high values for Ti and W, around 2 and 1 respectively and slowly evolve with T_e. The strong values obtained for Ti and W originate from the fact that the Fermi level lies within the d block, even when T_e increases. Excitation effects directly involves population or depopulation of localized d electronic states with strong impact on C_e. With a Fermi energy located on the top of the d block at low electronic temperature, a similar effect should also be observed for Ni, but this is actually hidden by the fit on large range of electronic temperatures. As we will see later, this phenomenon becomes visible when the fit is performed at lower temperatures. For W, once α_d is obtained from calculations that neglect the effect of semicore electrons, it is then possible to use this value to derive α_{sc} from the C_e curve obtained by taking into account the $4f^{14}$ electrons (GGAsc curve in Fig. 1(f)). This leads to a new fit in the high temperature limit, with N_e^{eff} being equal to 9. Accordingly, α_{sc} equals to 0 at low temperature and reaches the value of 0.2 at high temperature, confirming the effect of these electrons on C_e, assuming they are thermalized.

Since C_e is supposed to evolve linearly in the low temperature regime, it is often characterized by the electronic heat capacity coefficient $\gamma = C_e/T_e$. Values at 5×10^3 K are provided in Table 3, where a relative good agreement is found between calculated values and the low temperature free electron limit γ^l based on N_e^{eff}. However, for Ni the linear evolution of C_e is not respected, and a strong change of the slope occurs at low temperature. At T_e equals to 300 and 10^3 K, the corresponding γ values reach 1183.3 and 631.1 J K^{-2} m^{-3} respectively. In the low temperature limit, this involves very high values of N_e^{eff}, 19 and 10 respectively, leading to activity coefficients of d electrons of 2.1 and 1.0 respectively. This strong change of C_e slope at low temperature corresponds to a major difference in the behavior of Ni compared to Cu and Au. This difference of behavior originates from the position of the Fermi level, at the top of the d block for Ni while it is higher for Cu and Au, due to difference in their number of valence electrons. Thus, at low temperature, depopulation of the d block is direct for Ni, while the d block is not impacted yet for Cu and Au. When T_e increases, the Fermi level shift toward energies higher than the d block for both elements, inducing a strong changes of α_d in case of Ni, that progressively tends toward the values of Cu and Au. As in the case of Ti and W, a direct impact of the Fermi smearing on the d block has a strong effect on C_e which is signalled by important activity coefficient of localized d electrons. To a lower degree, a similar deviation is observed for Ti around $T_e = 10^3$ K, with a γ coefficient reaching the value of 466.3 J K^{-2} m^{-3}. This is fitted by a value of N_e^{eff} equals to 8 and leads to an even higher α_d with the value of 2.5. For these elements, the non-linear evolution of C_e at low electronic temperatures leads to strong modifications of subsequent derived quantities. Thus, beyond these general observations, the evolution of these activity coefficients remains difficult to be evaluated accurately and values cannot be extrapolated to other elements or temperature regime.

Table 3. Coefficient of electronic heat capacity ($\gamma = C_e/T_e$, J K^{-2} m^{-3}), at 5×10^3 K.

	Al	Ni	Cu	Au	Ti	W
γ	110.4	320.0	243.9	141.1	340.9	266.8
γ^l	96.2	309.3	262.5	172.8	328.7	342.2

5. Conclusion

In this paper, the electronic heat capacities are obtained from first-principles calculations performed at finite electronic temperatures. The effect of exchange and correlation functional on this thermodynamic quantity is first discussed. At high electronic temperature a small difference is observed between LDA and GGA functionals that was attributed to different equilibrium lattice parameters. The impact of semicore electrons, is also tested and demonstrated at high temperature for $4f^{14}$ electrons of tungsten. This is dependent on the energy depth of the corresponding semicore electronic states and is mostly negligible even at high temperatures, except for W. Assuming negligible effects or lower thermalization times for these electrons, effect of semicore electrons were neglected in the present study. Electronic heat capacities are also compared to previous theoretical predictions obtained from electronic structures not relaxed with the electronic temperature, with a very good agreement up to 4×10^4 K. Beyond this temperature, the response of the electronic structure exhibits differences.

The obtained electronic heat capacities are then discussed in the framework of low and high temperature limits of a free electron approach. Both are based on a free electron number, which is modified up to an effective number of electrons in order to fit the theoretical values of C_e. This approach applies correctly to Al as a free electron metal, but a significant overestimation of free electron numbers is found for the transition metals. Assuming a collective contribution of localized electrons on the C_e evolution, d electrons where considered associated to an activity coefficient. The high values obtained for this coefficient tend to corroborate the fact that d electrons respond collectively to the electronic excitation. A strong effect is observed from the impact of Fermi smearing on d electrons, as showed for Ni at low temperature and Ti and W in the whole range of temperature. For W, at very high temperature, an important contribution of semicore electrons $4f$ is also deduced from this approach, assuming that they are thermalized. At high temperature, the change of the electronic screening is found to affect significantly the localized d electrons, with a global shift of the d-block, strengthening the collective behavior of these electrons.

Additionally, the non-linear effect of d electrons, which is shown by an important dispersion of their activity coefficient, illustrates their non-free behavior and their interactive nature. The large numbers of electrons needed to fit C_e evolution in the low and high temperature regime is a signature of localized electron influence, mostly d electrons but also semicore electrons at very high temperature. Consequently, an unique free electron number cannot encompass the complex evolution of the electronic heat capacity and localized electrons, especially d ones, have to be considered. This shows that the free electron number is only one of the components on the energy storage of an irradiated material, and that localized electrons contribute as well, to various degrees depending on the electronic temperature.

6. Acknowledgments

This work was supported by the ANR project DYLIPSS (ANR-12-IS04-0002-01) and by the LABEX MANUTECH-SISE (ANR-10-LABX-0075) of the Université de Lyon, within the program "Investissements d'Avenir" (ANR-11-IDEX-0007) operated by the French National Research Agency (ANR). Numerical calculations have been performed using resources from GENCI, project gen7041.

[1] A. Cavalleri, Femtosecond electron crystallography reveals the atomic structural changes that underpin a light-induced insulator-metal transition, Science **318** (2007) 755-756.
[2] E.G. Gamaly, The physics of ultra-short laser interaction with solids at non-relativistic intensities, Phys. Rep. **508** (2011) 91-243.
[3] M.E. Povarnitsyn, K.V. Khishchenko, P.R. Levashov, Phase transitions in femtosecond laser ablation, Appl. Surf. Sci. **255**, (2009) 5120-5124.
[4] V. Recoules, J. Clérouin, G. Zérah, P.M. Anglade, S. Mazevet, Effect of intense laser irradiation on the lattice stability of semiconductors and metals, Phys. Rev. Lett., **96** (2006) 055503.
[5] J.P. Colombier, F. Garrelie, N. Faure, S. Reynaud, M. Bounhalli, E. Audouard, R. Stoian, F. Pigeon, Effects of electron-phonon coupling and electron diffusion on ripples growth on ultrafast-laser-irradiated metals, J. Appl. Phys. **111** (2012) 024902.
[6] P. Lorazo, L.J. Lewis, M. Meunier, Thermodynamic pathways to melting, ablation, and solidification in absorbing solids under pulsed laser irradiation, Phys. Rev. B **73** (2006) 134108.
[7] J.P. Colombier, P. Combis, E. Audouard, R. Stoian, Guiding heat in laser ablation of metals on ultrafast timescales: an adaptive modeling approach on aluminum, New J. Phys. **14** (2012) 013039.
[8] V.V. Zhakhovsky, M.M. Budzevich, N.A. Inogamov, I.I. Oleynik, C.T. White, Two-zone elastic-plastic single shock waves in solids, Phys. Rev. Lett. **107** (2011) 135502.
[9] B.Y. Mueller, B. Rethfeld, Relaxation dynamics in laser-excited metals under nonequilibrium conditions, Phys. Rev. B **87** (2013) 035139.
[10] M.I. Kaganov, I.M. Lifshitz, L.V. Tanatarov, Relaxation between electrons and crystalline lattices, Sov. Phys. JETP **4** (1957) 173.
[11] S.I. Anisimov, B.L. Kapeliovich, T.L. Perel'man, Non-Hamiltonian approach to conformal quantum field theory Sov. Phys. JETP **39** (1974) 10-18.

[12] E. Bévillon, J.-P. Colombier, V. Recoules, R. Stoian, Free-electron properties of metals under ultrafast laser-induced electron-phonon nonequilibrium: a first-principles study, Phys. Rev. B, **89** (2014) 115117.
[13] Z. Lin, L.V. Zhigilei, Temperature dependences of the electron-phonon coupling, electron heat capacity and thermal conductivity in Ni under femtosecond laser irradiation, Appl. Surf. Sci. **253** (2007) 6295-6300.
[14] Z. Lin, L.V. Zhigilei, V. Celli, Electron-phonon coupling and electron heat capacity of metals under conditions of strong electron-phonon nonequilibrium, Phys. Rev. B **77** (2008) 075133.
[15] G.V. Sinko, N.A. Smirnov, A.A. Ovechkin, P.R. Levashov, K.V. Khishchenko, Thermodynamic functions of the heated electron subsystem in the field of cold nuclei, High Energy Density Phys. 9, (2013) 309-314.
[16] X. Gonze *et al.*, ABINIT: First-principles approach to material and nanosystem properties, Comput. Phys. Commun. **180** (2009) 2582-2615.
[17] P. Hohenberg, W. Kohn, Inhomogeneous electron gas, Phys. Rev. **136** (1964) B864-B871.
[18] W. Kohn, L.J. Sham, Self-consistent equations including exchange and correlation effects, Phys. Rev. **140** (1965) A1133-A1138.
[19] N.D. Mermin, Thermal properties of the inhomogeneous electron gas, Phys. Rev. **137** (1965) A1441-A1443.
[20] M. Torrent, F. Jollet, F. Bottin, G. Zerah, X. Gonze, Comput. Mater. Sci. **42** (2008) 337.
[21] H.J. Monkhorst, J.D. Pack, Special points for Brillouin-zone integrations, Phys. Rev. B **13** (1976) 5188-5192.
[22] J.P. Perdew, Y. Wang, Accurate and simple analytic representation of the electron-gas correlation energy, Phys. Rev. B **45** (1992) 13244-13249.
[23] J.P. Perdew, K. Burke, M. Ernzerhof, Generalized gradient approximation made simple, Phys. Rev. Lett. **77** (1996) 3865-3868.
[24] D.V. Fisher, Z. Henis, S. Eliezer, J. Meyer-Ter-Vehn, Core holes, charge disorder, and transition from metallic to plasma properties in ultrashort pulse irradiation of metals, Laser Part. Beams **24** (2006) 81-94.
[25] N.W. Ashcroft, N.D. Mermin, Solid State Physics (Holt, Rinehart and Winston, New York, (1976).

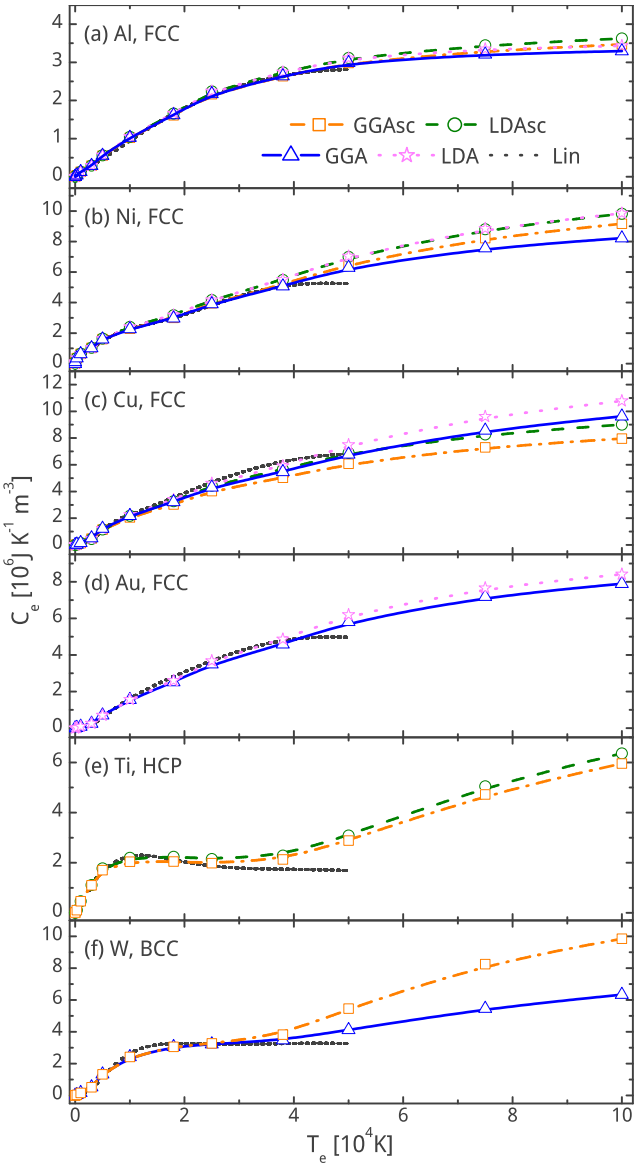

Figure 1. (Color online) Evolution of the electronic heat capacity with T_e for Al (a), Ni (b), Cu (c), Au (d), Ti (e), W (f), using different LDA and GGA exchange and correlation functionals. GGAsc and LDAsc indicate that the effect of semicore electrons are taken into account. The dotted black curves represent data of Lin *et al.* [14].

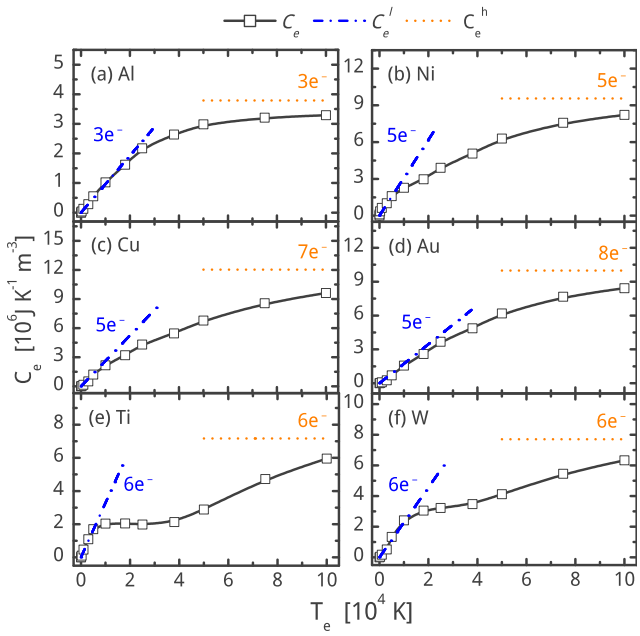

Figure 2. (Color online) Evolution of the electronic heat capacity with T_e for Al (a), Ni (b), Cu (c), Au (d), Ti (e), W (f), and its corresponding low and high temperature limits. The number of electrons used to fit the theoretical curve in both models is provided.

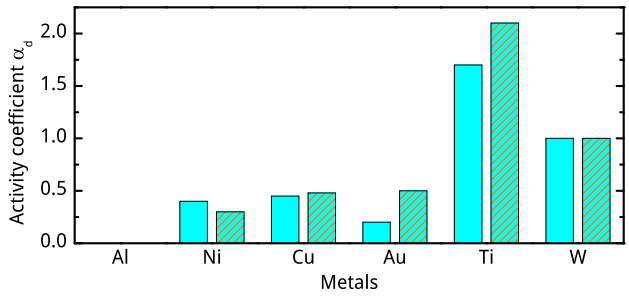

Figure 3. (Color online) Histogram representation of activity coefficients of localized d electrons. For each material, the left histogram corresponds to the low temperature case while the right one (patterned) represents the high temperature case.